partures from the model due to local processes, the thermal subsidence along the present-day convective motion direction follows the expected trend. Over the Pacific plate, the flow lines strongly differ from the age trajectories (Fig. 2), which is the key point to discriminate our analysis from previous models. Along the age trajectories, the depth profiles represented in Fig. 2 [based on a continuous grid (*23*)] show that there is an apparent flattening. But this flattening is only due to the misleading direction along which the subsidence is investigated. Contrary to previous models (*2*, *3*), our model fits the general trend of the bathymetry along the entire plate. The subsidence rates found in this study vary from 0.5 to 3.5 $m/m^{1/2}$. Rescaling by the constant Pacific plate velocity (9 cm $year^{-1}$) gives values ranging from 200 to 900 $m/Ma^{1/2}$, comparable to the values found in previous studies (*15*–*19*).

The general trend of the sea-floor depth along flow lines, representative of the underlying mantle convection, validates our hypothesis that the lithosphere should be viewed as the upper thermal boundary layer of mantle convection, its true definition (*26*). Because of the steady-state conditions imposed during the last 47 to 50 My (*24*), the Pacific lithosphere had time to readjust, by conduction, to the thermal conditions imposed at its base by the underlying convective mantle. The structure of the lithosphere (and, hence, its thermal subsidence) is therefore driven by the underlying mantle flow. This simple alternative perspective contrasts to the many more complicated explanations that have previously been proposed. In particular, we find that there is no sea-floor flattening at old ages and, therefore, no need to invoke any additional heat supply at the base of the old lithosphere.

References and Notes

1. J. G. Sclater, L. A. Lawver, B. Parsons, *J. Geophys. Res.* **80**, 1031 (1975).
2. B. Parsons, J. G. Sclater, *J. Geophys. Res.* **82**, 803 (1977).
3. C. A. Stein, S. Stein, *Nature* **359**, 123 (1992).
4. M.-P. Doin, L. Fleitout, *Earth Planet. Sci. Lett.* **142**, 121 (1996).
5. M.-P. Doin, L. Fleitout, *Geophys. J. Int.* **143**, 582 (2000).
6. R. L. Parker, D. W. Oldenburg, *Nature* **242**, 137 (1973).
7. A. G. Crosby, D. McKenzie, J. G. Sclater, *Geophys. J. Int.* **166**, 553 (2006).
8. B. Parsons, D. McKenzie, *J. Geophys. Res.* **83**, 4485 (1978).
9. D. A. Yuen, L. Fleitout, *Nature* **313**, 125 (1985).
10. M. A. Eberle, D. W. Forsyth, *Geophys. Res. Lett.* **22**, 473 (1995).
11. J. Huang, S. Zhong, *J. Geophys. Res.* **110**, B05404 (2005).
12. W. Schroeder, *J. Geophys. Res.* **89**, 9873 (1984).
13. G. F. Davies, *J. Geophys. Res.* **93**, 10467 (1988).
14. G. F. Davies, M. A. Richards, *J. Geol.* **100**, 151 (1992).
15. J. C. Marty, A. Cazenave, *Earth Planet. Sci. Lett.* **94**, 301 (1989).
16. B. Lago, A. Cazenave, J. C. Marty, *Phys. Earth Planet. Inter.* **61**, 253 (1990).
17. K. A. Kane, D. E. Hayes, *J. Geophys. Res.* **99**, 21759 (1994).
18. K. Perrot, J. Francheteau, M. Maia, C. Tisseau, *Earth Planet. Sci. Lett.* **160**, 593 (1998).
19. J. R. Cochran, W. R. Buck, *J. Geophys. Res.* **106**, 19233 (2001).
20. C. P. Conrad, C. Lithgow-Bertelloni, *J. Geophys. Res.* **109**, B10407 (2004).
21. S. R. Gaffin, B. C. O'Neill, *Geophys. Res. Lett.* **21**, 1947 (1994).
22. E. Humler, C. Langmuir, V. Daux, *Earth Planet. Sci. Lett.* **173**, 7 (1999).
23. Supporting material is available on *Science* Online.
24. W. D. Sharp, D. A. Clague, *Science* **313**, 1281 (2006).
25. A. E. Gripp, R. G. Gordon, *Geophys. Res. Int.* **150**, 321 (2002).
26. T. Turcotte, G. Schubert, *Geodynamics* (Cambridge Univ. Press, Cambridge, ed. 2, 2002).
27. W. H. F. Smith, D. T. Sandwell, *Science* **277**, 1956 (1997).
28. R. D. Müller, W. R. Roest, J.-Y. Royer, L. M. Gahagan, J. G. Sclater, *J. Geophys. Res.* **102**, 3211 (1997).

29. We thank A. Bonneville, F. Lucazeau, and Y. Fukao for fruitful discussions.

Supporting Online Material

www.sciencemag.org/cgi/content/full/328/5974/83/DC1
SOM Text
Figs. S1 and S2
References

14 December 2009; accepted 18 February 2010
10.1126/science.1185906

Orchestration of Floral Initiation by APETALA1

Kerstin Kaufmann,[1,2]* Frank Wellmer,[3]* Jose M. Muiño,[4] Thilia Ferrier,[5] Samuel E. Wuest,[3] Vijaya Kumar,[6] Antonio Serrano-Mislata,[7] Francisco Madueño,[7] Pawel Krajewski,[8] Elliot M. Meyerowitz,[6] Gerco C. Angenent,[1,9] José Luis Riechmann[5,6,10]†

The MADS-domain transcription factor APETALA1 (AP1) is a key regulator of *Arabidopsis* flower development. To understand the molecular mechanisms underlying AP1 function, we identified its target genes during floral initiation using a combination of gene expression profiling and genome-wide binding studies. Many of its targets encode transcriptional regulators, including known floral repressors. The latter genes are down-regulated by AP1, suggesting that it initiates floral development by abrogating the inhibitory effects of these genes. Although AP1 acts predominantly as a transcriptional repressor during the earliest stages of flower development, at more advanced stages it also activates regulatory genes required for floral organ formation, indicating a dynamic mode of action. Our results further imply that AP1 orchestrates floral initiation by integrating growth, patterning, and hormonal pathways.

Phase transitions in plants require the reprogramming of meristematic identities (*1*). Although several key regulators involved in this process have been identified, their molecular modes of action remain largely elusive. The floral meristem identity gene *APETALA1* (*AP1*) and its paralog *CAULIFLOWER* (*CAL*) control the onset of *Arabidopsis* flower development in a partially redundant manner (*2*). When both genes are mutated, plants do not transition to flowering but instead exhibit massive overproliferation of inflorescence meristems, leading to a cauliflower-like appearance. *AP1* expression is first observed throughout emerging floral primordia and is later confined to the outer whorls of floral buds, where AP1 is involved in the specification of sepals and petals (*3*). Several transcription factors have been identified that bind directly to the *AP1* promoter and control the onset of its expression. These include the floral meristem identity factor LEAFY (LFY) (*4*), the basic leucine zipper (bZIP) protein FD in concert with FLOWERING LOCUS T (FT) (*5*, *6*), as well as members of the SQUAMOSA PROMOTER BINDING PROTEIN-LIKE (SPL) family (*7*, *8*).

Previous studies have provided first insights into AP1 function during early flower development. AP1 directly represses the flowering time genes *SHORT VEGETATIVE PHASE* (*SVP*), *AGAMOUS-LIKE24* (*AGL24*), and *SUPPRESSOR OF OVEREXPRESSION OF CO1* (*SOC1*) in emerging floral primordia (*9*). Furthermore, it represses, directly or indirectly, the shoot identity gene *TERMINAL FLOWER1* (*TFL1*) (*10*), promotes the transcription of *LFY* as part of a positive feedback loop (*10*), and controls the expression of floral homeotic genes (*11*, *12*).

To obtain a detailed understanding of AP1 function during floral initiation, we identified genes that are controlled by it on a genome-wide scale. We used a previously described line expressing a fusion between AP1 and the hormone-binding domain of a glucocorticoid receptor (AP1-GR) in an *ap1 cal* double-mutant

[1]Business Unit Bioscience, Plant Research International, Wageningen 6700 AA, Netherlands. [2]Laboratory of Molecular Biology, Wageningen University, Wageningen 6700 AP, Netherlands. [3]Smurfit Institute of Genetics, Trinity College, Dublin 2, Ireland. [4]Applied Bioinformatics, Plant Research International, Wageningen 6700 AA, Netherlands. [5]Center for Research in Agricultural Genomics (CRAG), Barcelona 08034, Spain. [6]California Institute of Technology, Division of Biology, Pasadena, CA 91125, USA. [7]Instituto de Biología Molecular y Celular de Plantas, Consejo Superior de Investigaciones Científicas–Universidad Politécnica de Valencia, Valencia 46022, Spain. [8]Institute of Plant Genetics, Polish Academy of Sciences, Poznan 60-479, Poland. [9]Centre for BioSystems Genomics (CBSG), Wageningen 6700 AB, Netherlands. [10]Institució Catalana de Recerca i Estudis Avançats, Barcelona 08010, Spain.

*These authors contributed equally to this work.
†To whom correspondence should be addressed. E-mail: jriechma@caltech.edu

Downloaded from https://www.science.org at Copyright Clearance Center - Get It Now on August 06, 2025

Tecan Ex. 2115, Page 1 of 5
QIAGEN Sciences, LLC v. Tecan Genomics - IPR2025-00029

background (*13*). Activation of AP1-GR through treatment with dexamethasone leads to the simultaneous transformation of the inflorescence-like meristems of *ap1 cal* plants into floral primordia. We employed two microarray platforms (*14*) to identify genes that transcriptionally respond within 12 hours after AP1 activation (Fig. 1A) and identified 1366 genes that showed robust expression changes (with a fold change of >1.8 and adjusted *P* value of <0.05) (table S1). Because this set of genes should comprise both direct and indirect targets, we used the same AP1-GR system in chromatin immunoprecipitation (ChIP) experiments with AP1-specific antibodies followed by deep-sequencing (ChIP-Seq) (Fig. 1A and fig. S1) to determine AP1-binding sites on a genome-wide scale. We identified 1942 genomic regions that were significantly enriched in the dataset [with a false discovery rate (FDR) of <0.001] (table S2). In agreement with the observation that these regions were bound by AP1, we found that CArG boxes, the canonical binding motif of MADS-domain transcription factors (*15*), were highly enriched in these sequences (fig. S2). Analysis of the spatial distribution of AP1-binding sites further revealed that they are preferentially located near the transcriptional start site of genes (Fig. 1F). To define a set of potential AP1 targets, we searched for genes that contained one or more binding sites within 3 kb upstream of the 5′ end and 1 kb downstream of the 3′ end of the gene. Using these criteria, we identified 2298 genes as putative AP1 targets (table S2).

It has been demonstrated that in eukaryotes, transcription factor–binding events do not always coincide with changes in transcriptional activity (*16*). A comparison of the microarray and ChIP-Seq results revealed that approximately half (~44%) of the genes in proximity to AP1-binding sites showed expression changes after AP1 activation (fig. S3). However, the transcriptional response of many of these genes was small, and only 249 genes (which we refer to as high-confidence targets) showed robust (>1.8-fold) differential expression (tables S3 and S4). Quantitative reverse transcription polymerase chain reaction and independent ChIP experiments for selected genes confirmed the microarray and ChIP-Seq data (figs. S4 and S5), indicating that the limited overlap between the ChIP-Seq and microarray-selected gene sets was not a result of the methods used.

In agreement with the conjecture that early-response genes are more likely direct AP1 targets than late-response genes (which may include many secondary targets), most of the high-confidence targets were identified as differentially expressed in the earliest time points taken (Fig. 1E). Further evidence for a direct regulation of these genes by AP1 was provided by additional microarray analyses, for which we activated AP1 in the presence of the translational inhibitor cycloheximide (table S5). In these experiments, we found that 44% of the high-confidence targets responded transcriptionally in absence of protein biosynthesis. These results also illustrate the sufficiency of AP1 (in a floral context) to regulate its targets, whereas a comparison of gene expression between *ap1* mutant and wild-type inflorescences provided examples of its necessity for the regulation of high-confidence target genes (table S6).

Although AP1 has only minor or no effects on the expression of many of the genes near which it binds, the preferential location of binding sites in close proximity to transcriptional start sites (Fig. 1F and fig. S6) suggests that at least a subset of these sites may mediate transcriptional responses. Whereas weak transcriptional responses might indicate a role of AP1 in fine-tuning gene expression, some of the genes that did not respond in our experiments may do so when additional cofactors are present. In agreement with this idea, a fraction of those genes showed robust changes in

Downloaded from https://www.science.org at Copyright Clearance Center - Get It Now on August 06, 2025

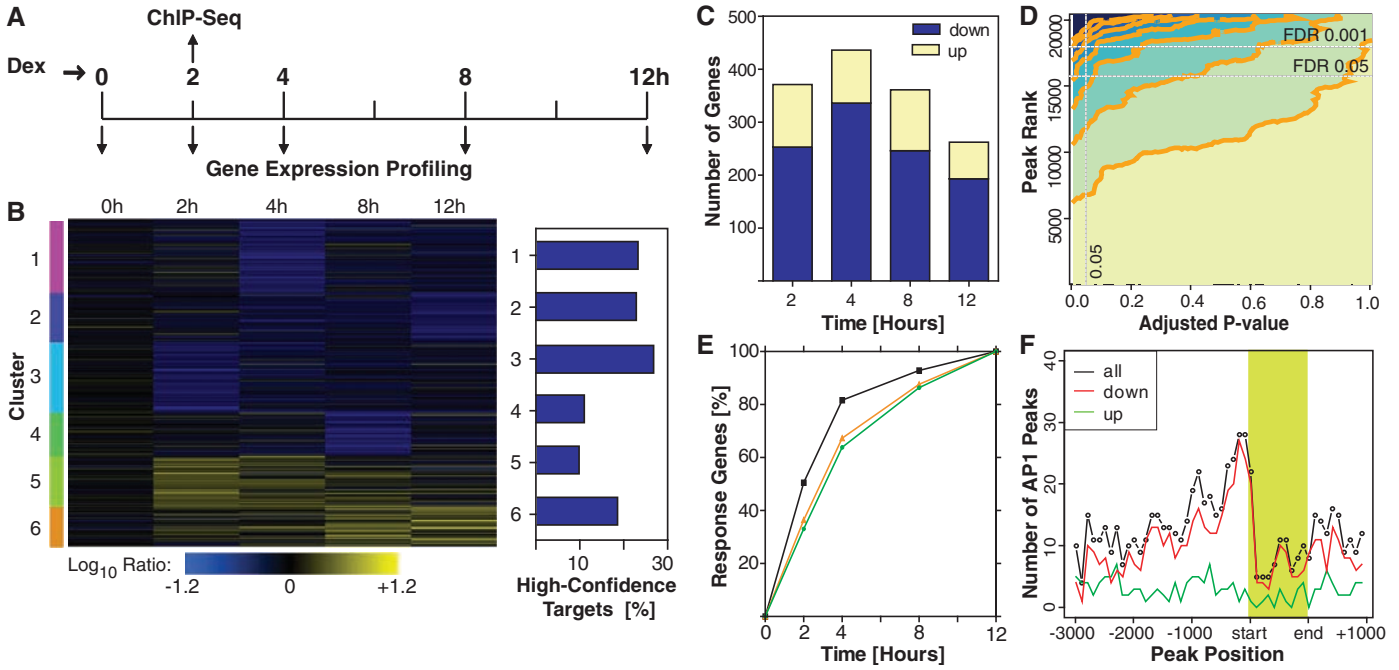

Fig. 1. Overview of results from microarray (Agilent, Santa Clara, California) and ChIP-Seq analyses. (**A**) Experimental setup. (**B**) Gene expression changes after AP1 activation. Cluster analysis was performed by using $\log_{10}$ ratios for 1017 response genes identified by means of microarray analysis. The fraction of high-confidence targets in each cluster is indicated on the right. (**C**) Gene expression changes at different time points after AP1 activation. The numbers of genes that were up- or down-regulated are shown. (**D**) Contour plot showing the relationship between the rank of ChIP-Seq peaks and the adjusted *P* values for differential expression (2-hour time point). Horizontal and vertical white lines indicate FDR and *P* value thresholds, respectively. (**E**) Fraction of response genes identified at different times after AP1 activation. Colored lines indicate results for all response genes (orange), high-confidence targets (black), and response genes excluding high-confidence targets (green). (**F**) Spatial distribution and number of ChIP-Seq peaks in proximity to transcribed regions of differentially expressed genes (identified in the 2-hour time point). To account for different gene sizes, the positions of binding sites within transcribed regions (shaded in green) were calculated relative to their lengths. Colored lines represent results for all differentially expressed genes and genes that were either down- or up-regulated (as indicated).

Tecan Ex. 2115, Page 2 of 5
QIAGEN Sciences, LLC v. Tecan Genomics - IPR2025-00029

expression at more advanced stages of flower development (fig. S7) when AP1-GR nuclear accumulation still persisted (fig. S8). Furthermore, members of the family of MADS-domain transcription factors share similar DNA-binding specificities (*15*). Therefore, AP1 might be able to bind to sites that become functional only when they are occupied by other MADS-domain proteins.

Among the high-confidence AP1 targets, we found a strong enrichment of transcription factor–coding genes (25% as compared with ~6% genome-wide) (*17*) (fig. S9 and table S7), indicating that AP1 mediates floral initiation to a large extent by controlling the expression of other transcriptional regulators. Among these genes, several are known to be involved in the control of *AP1* expression. An example is *LFY*, which is directly up-regulated by AP1 (Fig. 2), indicating that the positive feedback loop between AP1 and LFY is mediated by direct interactions. AP1 also represses the flowering time gene *FD*, which is known to be involved in the activation of *AP1* in incipient floral primordia, and its paralog *FDP*. This result is in agreement with the observation that *FD* is repressed at stage 2 of flower development (*5*) and thus shortly after *AP1* expression commences. In a similar fashion, AP1 represses *SPL9*, which encodes another direct activator of *AP1* that is down-regulated in stage 2 flowers (*7*), and its paralog *SPL15* (fig. S10).

We also found that several genes encoding members of the AP2 family of transcription factors, which had been shown previously to act as floral repressors (*18*–*20*), were down-regulated by AP1 (Fig. 2). These include *TARGET OF EAT1* (*TOE1*), *TOE3* and *SCHNARCHZAPFEN* (*SNZ*) but not the closely related *TOE2* or *SCHLAFMÜTZE* (*SMZ*) (fig. S4). It has been suggested that the corresponding factors act redundantly and may prevent flowering in part by directly repressing *AP1* (*20*). Thus, AP1 appears to counteract its own suppression by down-regulating these genes. AP1 also down-regulates *TEMPRANILLO1* (*TEM1*) and *TEM2* (Fig. 2), which code for related transcription factors that contribute to the regulation of flowering through the repression of *FT* expression in leaves (*21*). The finding that these genes are directly repressed by AP1 suggests an additional function for *TEM1*/*TEM2* in the inflorescence meristem. Lastly, we found that AP1 represses the known AP1 antagonist *TFL1* and binds to at least two sites in the 3′ region of the gene (Fig. 2A). The results of genetic analyses confirmed that the region 3′ to *TFL1* is required for proper *TFL1* activity (Fig. 3 and table S8), although we currently do not know whether the AP1-binding sites we identified in it are essential. Taken together, these results indicate that AP1 controls a complex gene regulatory module that ensures and fine-tunes its own expression and that suppresses floral-repressor and shoot-identity genes in emerging floral primordia (Fig. 2 and fig. S10). Furthermore, a global analysis of gene expression changes after AP1 activation revealed that more than 80% of AP1 targets were down-regulated (Fig. 1, B and C, and table S1), indicating that AP1 acts predominantly as a transcriptional repressor during floral initiation.

Shortly after the onset of flower formation, the flowering time genes *AGL24* and *SVP* are down-regulated by AP1 (*9*). Because AGL24 and SVP repress *SEP3*, their down-regulation leads to the induction of *SEP3* expression at stage 2 of flower development (*22*). In addition, AP1 binds to the *SEP3* promoter, and *SEP3* expression is rapidly up-regulated after AP1 activation (fig. S10). Thus, AP1 appears to promote *SEP3* expression through both direct and indirect mechanisms.

It has been proposed that the induction of *SEP3* and the concomitant down-regulation of *AGL24* and *SVP* during early flower development lead to the formation of AP1/SEP3 heterodimers (*11*, *22*, *23*), which are then involved in the activation of floral homeotic genes required for floral organ formation. To test this idea, we compared the ChIP-Seq data for AP1 with those recently obtained for SEP3 in whole inflorescences (*24*). This comparison revealed a large overlap between both their putative target genes (~64% of all genes bound by AP1 also contain SEP3-binding sites) and location of their binding sites (Fig. 4, A and B, and fig. S11), strongly suggesting that they indeed preferentially act together in transcriptional complexes.

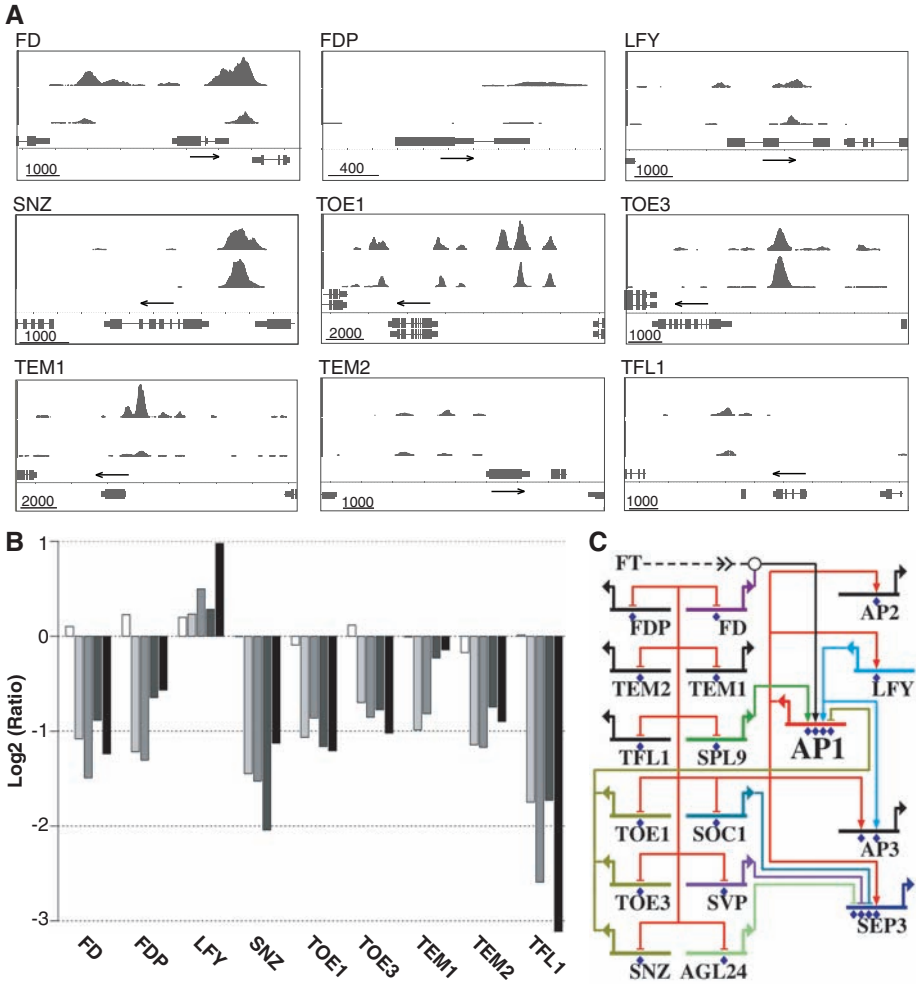

Fig. 2. Selected AP1 target genes. (**A**) ChIP-Seq results for selected targets (as indicated). In each panel, the topmost trace represents AP1 ChIP-Seq data followed by those for SEP3 (*24*), which are shown for comparison. Genes found in the genomic regions analyzed, as well as their exon-intron structure, are indicated in the bottom half of each panel. Scale bars indicate sequence lengths [in base pairs (bp)], and arrows indicate gene orientations. The scale of the *y* axis (peak height) is adjusted for individual traces for visual clarity. (**B**) Transcriptional responses of the genes shown above after AP1 activation. The plot was generated by using $\log_2$ ratios derived from Operon (Huntsville, Alabama) (*TEM2*) and Agilent (all other genes) microarray experiments. Time points are 0 (white bars), 2, 4, 8 (gray scale), and 12 hours (black bars). (**C**) Gene-regulatory network controlled by AP1 during floral initiation. Only selected targets are shown. Arrows indicate gene activation, and blunted lines indicate repression. Blue dots underneath gene symbols indicate direct regulation. The diagram was generated with BioTapestry (*29*).

Downloaded from https://www.science.org at Copyright Clearance Center - Get It Now on August 06, 2025

Tecan Ex. 2115, Page 3 of 5
QIAGEN Sciences, LLC v. Tecan Genomics - IPR2025-00029

We further found that common targets of SEP3 and AP1 showed a strong enrichment for genes that are activated during floral organ initiation (Fig. 4C). Thus, AP1/SEP3 heterodimers appear to function predominantly, but not exclusively (*11*, *25*), as transcriptional activators during early flower development.

Floral primordia are initiated at the flanks of the inflorescence meristem. The morphological changes associated with flower primordium formation suggested a possible role of AP1 in regulating cell proliferation. In agreement with this idea, we found that AP1 directly controls the expression of genes with known functions in the control of organ growth. Examples are genes involved in the metabolism of and response to the hormone gibberellin (GA), which affects both cell elongation and proliferation (*26*). AP1 up-regulates *GA3ox1*, which encodes a key enzyme involved in GA biosynthesis. Conversely, AP1 promotes expression of *GA2ox1*, which encodes a GA catabolic enzyme, as well as of *RGA-LIKE2*, which is a known repressor of GA response. Thus, AP1 appears to mediate GA homeostasis in floral primordia through complex interactions. AP1 also directly regulates the expression of genes involved in patterning processes. An example is *ARABIDOPSIS THALIANA HOMEOBOX GENE1*, which is involved in boundary formation (*27*) and has been shown to be also a target of the floral homeotic factor AGAMOUS during the formation of the reproductive floral organs (*28*).

Our results suggest distinct functions of AP1 during the initiation of flower development. AP1 appears to establish floral meristem identity by repressing genes that are part of the shoot developmental program or that control the onset of flowering in part by activating *AP1* itself. It also seems to orchestrate the formation of floral primodia by regulating genes involved in organ growth and patterning. Lastly, at more advanced stages of flower development AP1 initiates downstream pathways required for floral organ specification, most likely in combination with SEP3. Thus, AP1 acts as a true hub in the regulatory network that mediates the switch from floral induction to flower formation.

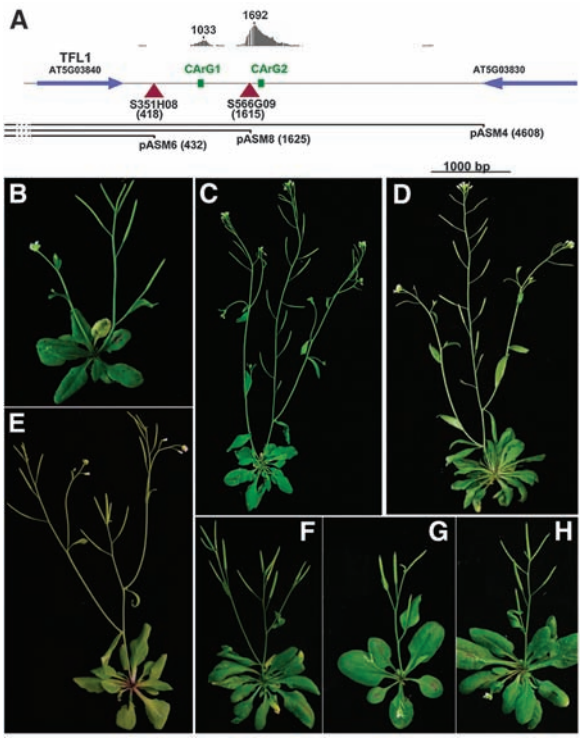

Fig. 3. The genomic region downstream of *TFL1* is required for its function. (**A**) Diagram depicting the *TFL1* genomic region. Coordinates are relative to the last position of the *TFL1* stop codon. Blue arrows indicate gene orientation, green boxes mark two CArG boxes (at positions 1011 and 1756) within AP1 ChIP-Seq peaks, and purple arrowheads indicate the positions of T-DNA insertions. Black lines represent the genomic fragments used for complementation experiments (as indicated). (**B**) *tfl1-1* mutant. The primary inflorescence forms a terminal flower, and secondary inflorescences are replaced by solitary flowers. (**C**) Wild-type plant. Primary and secondary inflorescences show indeterminate growth. (**D**) *tfl1-1* mutant fully rescued by transformation with pASM4. (**E**) *tfl1-1* mutant partially rescued after transformation with pASM8, which lacked one of the AP1-binding sites. (**F**) Plant homozygous for a T-DNA insertion 1615 bp downstream of the *TFL1* stop codon. Although more severe, its phenotype overall resembled that of *tfl1-1* pASM8 plants. (**G**) *tfl1-1* mutant not rescued after transformation with pASM6, which lacked both AP1-binding sites. (**H**) Plant homozygous for a T-DNA insertion 418 bp downstream from the *TFL1* stop codon showing a *tfl1-1* mutant phenotype.

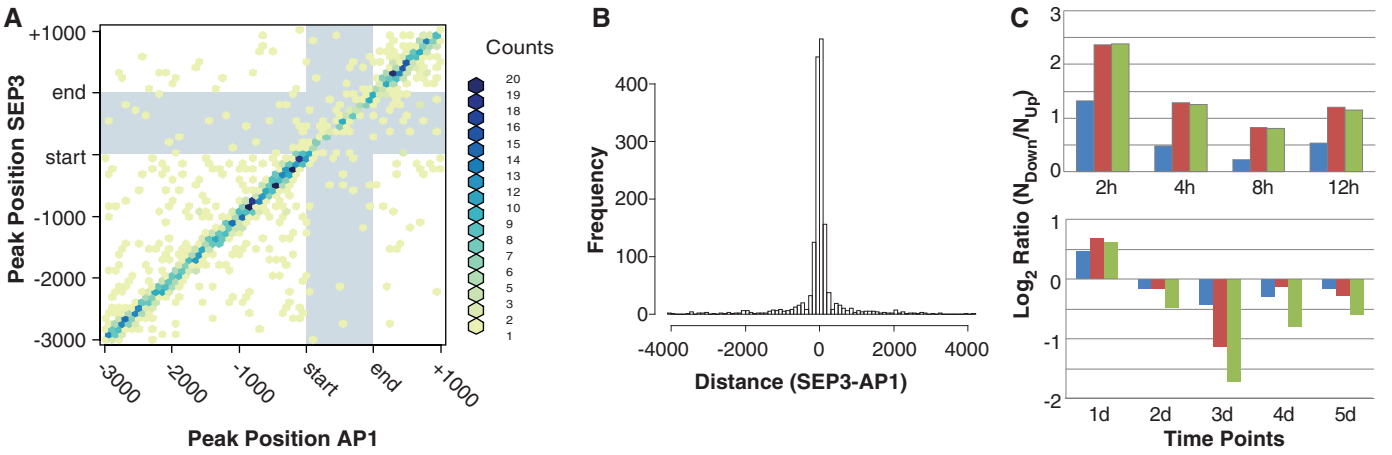

Fig. 4. Spatial distribution of AP1- and SEP3-binding sites. (**A**) Position of SEP3- and AP1-paired ChIP-Seq peaks in common target genes. The paired AP1 peaks depicted in this diagram represent ~87% of all AP1 peaks detected in the set of common target genes (*14*). Binding data for SEP3 were taken from (*24*). Transcribed regions are shaded in gray. Within transcribed regions, peak positions were calculated as a fraction of the gene length (Fig. 1F). The density of peak pairs in the graph is represented with a color scale (counts are the number of peak pairs per area unit). (**B**) Distance distribution of SEP3- and AP1-binding sites in common target genes. Each bar represents a 100-bp window. (**C**) Differential expression of AP1 and SEP3 target genes during early flower development. Log_2 ratios for the number of down- and up-regulated genes were calculated for a given time point after AP1 activation (as indicated). Gene sets analyzed included all differentially expressed genes (blue bars), genes bound by AP1 (red bars), and genes bound by both AP1 and SEP3 (green bars). Expression data analyzed for the bottom panel were taken from (*13*), and the top panel displays data obtained with the same microarray platform (Operon).

Downloaded from https://www.science.org at Copyright Clearance Center - Get It Now on August 06, 2025

Tecan Ex. 2115, Page 4 of 5
QIAGEN Sciences, LLC v. Tecan Genomics - IPR2025-00029

References and Notes

1. G. Chuck, S. Hake, *Curr. Opin. Plant Biol.* **8**, 67 (2005).
2. C. Ferrándiz, Q. Gu, R. Martienssen, M. F. Yanofsky, *Development* **127**, 725 (2000).
3. M. A. Mandel, C. Gustafson-Brown, B. Savidge, M. F. Yanofsky, *Nature* **360**, 273 (1992).
4. D. Wagner, R. W. Sablowski, E. M. Meyerowitz, *Science* **285**, 582 (1999).
5. P. A. Wigge *et al.*, *Science* **309**, 1056 (2005).
6. M. Abe *et al.*, *Science* **309**, 1052 (2005).
7. J. W. Wang, B. Czech, D. Weigel, *Cell* **138**, 738 (2009).
8. A. Yamaguchi *et al.*, *Dev. Cell* **17**, 268 (2009).
9. C. Liu *et al.*, *Development* **134**, 1901 (2007).
10. S. J. Liljegren, C. Gustafson-Brown, A. Pinyopich, G. S. Ditta, M. F. Yanofsky, *Plant Cell* **11**, 1007 (1999).
11. V. Gregis, A. Sessa, C. Dorca-Fornell, M. M. Kater, *Plant J.* **60**, 626 (2009).
12. M. Ng, M. F. Yanofsky, *Plant Cell* **13**, 739 (2001).
13. F. Wellmer, M. Alves-Ferreira, A. Dubois, J. L. Riechmann, E. M. Meyerowitz, *PLoS Genet.* **2**, e117 (2006).
14. Materials and methods are available as supporting material on *Science* Online.
15. J. L. Riechmann, M. Wang, E. M. Meyerowitz, *Nucleic Acids Res.* **24**, 3134 (1996).
16. X. Y. Li *et al.*, *PLoS Biol.* **6**, e27 (2008).
17. J. L. Riechmann *et al.*, *Science* **290**, 2105 (2000).
18. M. J. Aukerman, H. Sakai, *Plant Cell* **15**, 2730 (2003).
19. M. Schmid *et al.*, *Development* **130**, 6001 (2003).
20. J. Mathieu *et al.*, *PLoS Biol.* **7**, e1000148 (2009).
21. C. Castillejo, S. Pelaz, *Curr. Biol.* **18**, 1338 (2008).
22. C. Liu, W. Xi, L. Shen, C. Tan, H. Yu, *Dev. Cell* **16**, 711 (2009).
23. V. Gregis, A. Sessa, L. Colombo, M. M. Kater, *Plant J.* **56**, 891 (2008).
24. K. Kaufmann *et al.*, *PLoS Biol.* **7**, e1000090 (2009).
25. V. V. Sridhar, A. Surendrarao, Z. Liu, *Development* **133**, 3159 (2006).
26. P. Achard *et al.*, *Curr. Biol.* **19**, 1188 (2009).
27. C. Gómez-Mena, R. Sablowski, *Plant Cell* **20**, 2059 (2008).
28. C. Gómez-Mena, S. de Folter, M. M. Costa, G. C. Angenent, R. Sablowski, *Development* **132**, 429 (2005).
29. W. J. Longabaugh, E. H. Davidson, H. Bolouri, *Dev. Biol.* **283**, 1 (2005).
30. We are grateful to T. Mastro for help with microarray hybridizations, S. Kushnir for generating AP1 antibodies, Y. Hanzawa and D. Bradley for providing transferred DNA (T-DNA) insertion lines, and E. Graciet for help with AP1-GR detection in nuclear extracts. This work was supported by grants from Science Foundation Ireland (06/IN.1/B851 to F.W.), European Union (EU)–Marie Curie program (Transistor-MRTNCT-2004–512285 to G.C.A. and IRG-224864 to J.L.R.), NSF (2010-0520193 to J.L.R. and E.M.M.), Spanish Ministerio de Ciencia e Innovación (BFU2008-04251 to J.L.R. and BIO2006-10994 and BIO2009-10876 to F.M.), and by the Millard and Muriel Jacobs Laboratory at Caltech. G.C.A. was also supported by the Netherlands Proteomics Centre and CBSG, which are part of the Netherlands Genomic Initiative. K.K. and J.M.M. were supported by fellowships from the EU–Marie Curie program; J.M.M. was also supported by CBSG and a Horizon grant (#93519020). T.F. was supported by a fellowship from CRAG. Microarray data have been deposited with the National Center for Biotechnology Information Gene Expression Omnibus under accession numbers GSE20184 and GSE20138 and the sequencing data under accession number GSE20176.

Supporting Online Material

www.sciencemag.org/cgi/content/full/328/5974/85/DC1
Materials and Methods
Figs. S1 to S11
Tables S1 to S12
References

26 November 2009; accepted 4 March 2010
10.1126/science.1185244

Maize Tumors Caused by *Ustilago maydis* Require Organ-Specific Genes in Host and Pathogen

David S. Skibbe,[1]* Gunther Doehlemann,[2]* John Fernandes,[1] Virginia Walbot[1]†

Infection of maize by corn smut (*Ustilago maydis*) provides an agronomically important model of biotrophic host-pathogen interactions. After penetration of the maize epidermis, fungal colonization of host tissue induces tumor formation on all aerial maize organs. We hypothesized that transformation of different primordia into plant tumors would require organ-specific gene expression by both host and pathogen and documented these differences by transcriptome profiling. Phenotypic screening of *U. maydis* mutants deleted for genes encoding secreted proteins and maize mutants with organ-specific defects confirmed organ-restricted tumorigenesis. This is the foundation for exploring how individual pathogen effectors, deployed in an organ-specific pattern, interact with host factors to reprogram normal ontogeny into a tumor pathway.

Ustilago maydis, the causal agent of corn smut disease, is a basidiomycete fungus parasitizing only maize and its wild progenitor teosinte (both *Zea mays* L.) (*1*). *U. maydis* elicits large tumors on all aerial organs, where it completes pathogenic development by forming teliospores, its predominant dispersal agent (*1*). Unlike oncogenic agents that reactivate cell division, *U. maydis* is tumorigenic because fungal signals subvert normal programming of proliferating host cells, resulting in an extended period of plant cell division, chromosome endoreduplication, and cell expansion (*2*).

During the arms race with the multilayered plant defense system, plant pathogens such as *U. maydis* evolved a broad molecular repertoire to establish a compatible interaction (*3*). In contrast to necrotrophic pathogens that kill invaded cells and feed on debris, biotrophic pathogens establish an intimate interaction with living hosts (Fig. 1, A and B) by suppressing plant defenses while tapping the nutritional supply of colonized cells. This interaction is maintained by secretion of fungal effector proteins, which either act at the biotrophic interface between pathogen and plant cell or are translocated into the host cytoplasm (*3*). Sequencing of the *U. maydis* genome and transcriptome profiling during seedling infection identified 12 gene clusters encoding primarily uncharacterized, predicted secreted proteins expressed in planta (*4*). Infection assays with maize seedlings identified five of these clusters as functionally involved in tumor formation (*4*).

Extensive analysis of bacterial and oomycete effector proteins has identified several mechanisms for host cell manipulation (*5*); however, to date there is no evidence that the action or expression of any pathogen effector is tailored to individual host tissues. This is surprising because *U. maydis* is tumorigenic in leaves, stems, and flowers, and these organs and constituent maize tissues and cell types express distinctive developmental genes (*6*), as is true in any complex eukaryote. Furthermore, maize mutations that disrupt normal development can enhance or suppress tumor progression (*7*), demonstrating that host developmental status is important in the biotrophic interaction.

To define the genes expressed by maize and *U. maydis* during infections culminating in tumors (Fig. 1, C and D), transcriptomes were assessed on a microarray with probes to ~6700 annotated *U. maydis* genes (*4*), 4941 of which showed only background levels of hybridization with maize RNA in control hybridizations (i.e., high-confidence probes), and 36,800 maize genes, representing most gene models (*8*). Water-injected (mock infection) and fungal-infected organs were evaluated at 1 and 3 dpi (days postinjection) in seedling leaves and at 3 and 9 dpi in adult leaves and tassels (male reproductive inflorescences), as diagrammed in Fig. 1E (*9*).

Confirming previous reports (*10*, *11*), more than 30,000 maize genes were constitutively expressed (from mock 3-dpi samples), plus over 1500 organ-specific genes (table S1). Combined data from all three organs, comparing infected to mock samples, showed that 9207 (25%) unique maize transcripts were up-regulated (Fig. 2A) and 4455 (12%) were expressed only during fungal infection (Fig. 2B). At 3 dpi, *U. maydis* infection altered about one-third of the seedling leaf transcriptome: 4041 types were up-regulated or detected only in the infected sample ("on") (Fig. 2A), and 8111 transcript types were down-regulated or not detected in the infected sample ("off") (Fig. 2C). In adult leaves, more genes were up-regulated or on (6339) (Fig. 2A) than were down-regulated or off (3899) (Fig. 2C). In tassels,

[1]Department of Biology, Stanford University, Stanford, CA 94305–5020, USA. [2]Max Planck Institute for Terrestrial Microbiology, D-35043 Marburg, Germany.

*These authors contributed equally to this work.
†To whom correspondence should be addressed. E-mail: walbot@stanford.edu

Downloaded from https://www.science.org at Copyright Clearance Center - Get It Now on August 06, 2025

Tecan Ex. 2115, Page 5 of 5
QIAGEN Sciences, LLC v. Tecan Genomics - IPR2025-00029